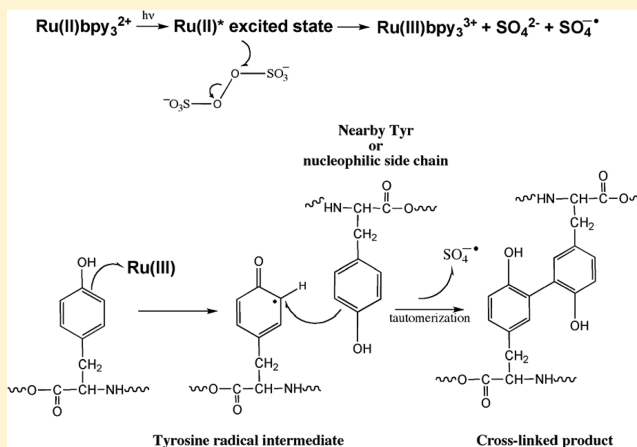


# Continuous Flow Reactor for the Production of Stable Amyloid Protein Oligomers

Eric Yale Hayden and David B. Teplow\*

Department of Neurology, David Geffen School of Medicine at UCLA, Neuroscience Research Building, Room 445, 635 Charles E. Young Drive South, Los Angeles, California 90095-7334, United States

**ABSTRACT:** The predominant working hypothesis of Alzheimer's disease is that the proximate pathologic agents are oligomers of the amyloid  $\beta$ -protein ( $A\beta$ ). "Oligomer" is an ill-defined term. Many different types of oligomers have been reported, and they often exist in rapid equilibrium with monomers and higher-order assemblies. This has made formal structure–activity determinations difficult. Recently, Ono et al. [Ono, K., et al. (2009) *Proc. Natl. Acad. Sci. U.S.A.* 106, 14745–14750] used rapid, zero-length, in situ chemical cross-linking to stabilize the oligomer state, allowing the isolation and study of pure populations of oligomers of a specific order (number of  $A\beta$  monomers per assembly). This approach was successful but highly laborious and time-consuming, precluding general application of the method. To overcome these difficulties, we developed a "continuous flow reactor" with the ability to produce theoretically unlimited quantities of chemically stabilized  $A\beta$  oligomers. We show, in addition to its utility for  $A\beta$ , that this method can be applied to a wide range of other amyloid-forming proteins.



Alzheimer's disease (AD) is the most common age-related dementia, affecting more than 5.3 million in the United States alone.<sup>1</sup> This number is expected to triple by 2050.<sup>2</sup> A growing body of evidence suggests that oligomeric forms of the amyloid  $\beta$ -protein,  $A\beta$ , may be the proximate neurotoxins in AD.<sup>3</sup> Oligomeric assemblies have been shown to exist at increased concentrations in vivo in AD patients and in AD animal models.<sup>4,5</sup> These oligomers are associated with significant neuronal dysfunction before any amyloid deposits are observed.<sup>6</sup> In addition, rats injected with oligomeric  $A\beta$  assemblies display significant inhibition of hippocampal long-term potentiation, a measure of learning and memory.<sup>7</sup> In vitro studies have shown that  $A\beta$  oligomers are more toxic than either monomers or amyloid fibrils.<sup>8</sup> Similar findings with other diseases associated with amyloid-forming proteins have been published: Parkinson's disease<sup>9</sup> [ $\alpha$ -synuclein ( $\alpha$ Syn)], type II diabetes<sup>10,11</sup> [islet amyloid polypeptide (IAPP)], familial amyloid polyneuropathy<sup>12</sup> [transthyretin (TTR)], dialysis-related amyloidosis<sup>13</sup> [ $\beta_2$ -microglobulin ( $\beta_2$ M)], and medullary carcinoma of the thyroid<sup>14</sup> [calcitonin (CT)]. These observations have led to a paradigm shift in target identification for drug discovery, namely away from the importance of amyloid deposits and fibrils per se toward the central role of protein oligomers.

A complex equilibrium exists among monomers and oligomers that involves both monomer conformation (secondary and tertiary structure) and order (quaternary structure).<sup>3,15,16</sup> Various oligomer structures have been described,<sup>3</sup> but no consensus exists with respect to either oligomer structure or biological

activity, i.e., structure–activity (neurotoxicity) relationships (SAR). This fundamental problem exists because of the metastable and heterogeneous nature of oligomers.<sup>15</sup> For this reason, a detailed structural and functional characterization of the oligomers, particularly of the more toxic 42-amino acid form of  $A\beta$ ,  $A\beta_{42}$ , has proven to be difficult.<sup>17</sup>

To address the metastability problem, we used the method of photoinduced cross-linking of unmodified proteins (PICUP) to "freeze" the oligomer population, allowing quantitative determination of the oligomer size frequency distribution.<sup>18</sup> When we originally published our application of the PICUP method in the  $A\beta$  system,<sup>19</sup> extensive control experiments showed that the technique accurately reflected the oligomer frequency distribution in solution at the moment of cross-linking, for system sizes of <20 monomers per oligomer. This system size appears to be the one most likely to contribute to the pathogenesis of AD, as suggested by many (for a review, see ref 3). The data were consistent with studies of assembly size conducted using dynamic light scattering<sup>19</sup> and with later discrete molecular dynamics simulations of  $A\beta$  oligomerization.<sup>20</sup> The technique revealed that other amyloidogenic proteins yielded distinct oligomerization patterns whereas nonamyloidogenic, monomeric proteins yielded distributions consistent with concentration-dependent, diffusion-limited cross-linking,

Received: June 9, 2012

Revised: July 16, 2012

Published: July 17, 2012



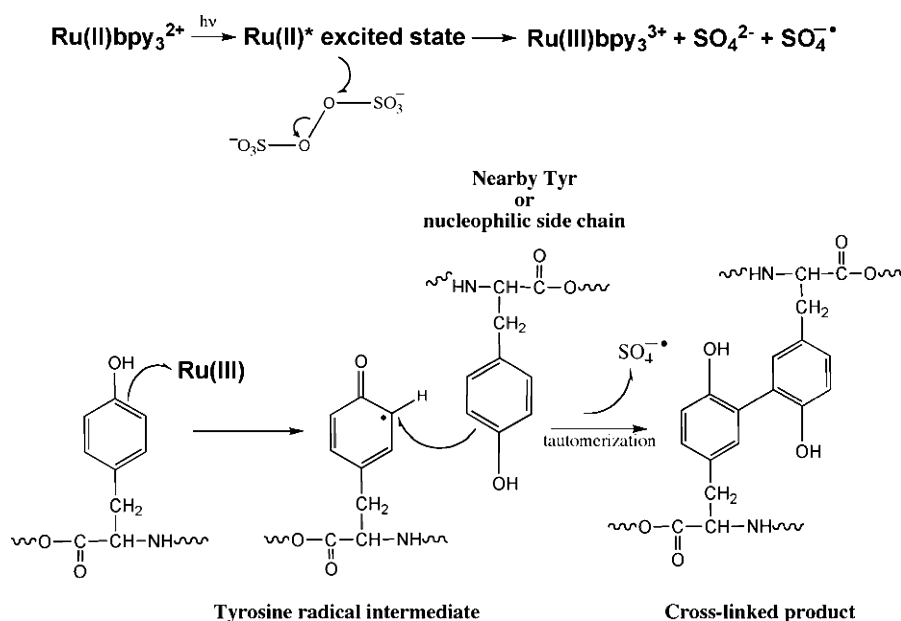


**Figure 1.** Photoinduced cross-linking of unmodified protein (PICUP). The chemistry is initiated by photolyzing Ru(II) ( $\lambda_{\text{max}} = 452 \text{ nm}$ ) with visible light. Photolysis of this metal complex produces an excited state, which can donate an electron to persulfate, cleaving its O–O bond. The products are Ru(III), the sulfate radical, and the sulfate anion. The activated metal complex Ru(III) can abstract an electron from a nearby amino acid (Tyr, Trp, His, or Met are the most reactive). This produces a protein radical species that can then attack a wide variety of other groups on nearby proteins. This chemistry results in a covalently cross-linked protein complex without any prior modification to the protein of interest.

namely, ladders of bands, the nodes of which were determined by protein concentration, as would be expected from random collision-induced cross-linking. These data provided further evidence that the cross-linking system does reflect what exists in solution.

Ono et al.<sup>17</sup> recently showed that the PICUP technique yielded stable, low-order A $\beta$ 40 oligomers of constant quaternary structure and restricted conformational complexity, which allowed the performance of formal SAR studies for monomers through tetramers. Although successful, the studies of Ono et al. required the laborious and time-consuming preparation of hundreds of small batches of each oligomer that were pooled to provide sufficient material for study. Such an analytical-scale process precludes production of the quantities of pure oligomers required for the broad range of studies necessary to fully characterize A $\beta$  oligomer structure [e.g., nuclear magnetic resonance (NMR) and X-ray crystallography], examine biological activity (in cell culture and animals), produce specific antibodies, or prepare oligomer immunogens for therapeutic purposes.

We report here that preparative-scale amounts of cross-linked A $\beta$  oligomers can be produced easily using a continuous flow reaction system. We show that other amyloid proteins also can be cross-linked successfully using this system. The ability to produce large quantities of stable oligomers should now allow a variety of biophysical and biological experiments that heretofore have been precluded because of sample scarcity and oligomer instability.

## EXPERIMENTAL PROCEDURES

A $\beta$  was prepared by the Biopolymer Laboratory at UCLA.  $\alpha$ Syn was a gift from the laboratory of D. Eisenberg. Other proteins were purchased from Sigma (TTR), Anaspec (CT), Poly Peptide (San Diego, CA) (IAPP), and Lee Biosolutions (St. Louis, MO) ( $\beta$ 2M). 1,1,1,3,3,3-Hexafluoro-2-propanol (HFIP) was obtained from TCI America (Portland, OR). Tris(2,2'-bipyridyl)-dichlororuthenium(II) hexahydrate [Ru(II)] and ammonium

persulfate (APS) were purchased from Sigma. Dithiothreitol (DTT) was purchased from Fisher.

**Preparation of LMW A $\beta$ .** Lyophilized A $\beta$  was dissolved in 60 mM NaOH, diluted into 1 volume of Milli-Q water, and then mixed with an equal volume of 22 mM sodium phosphate buffer (pH 7.4). The material was sonicated in an ultrasonic water bath (model 1510, Branson Ultrasonics Corp., Danbury, CT) for 1 min at 22 °C, transferred into centrifugal filters (30000 molecular weight cutoff, Centricon YM-30, Millipore Corp., Billerica, MA), and centrifuged at 16000g using a bench-top microcentrifuge (Eppendorf model 5415C, Brinkmann Instruments) for 30 min. The eluate from the filtration was collected, and A $\beta$  was quantified by UV absorbance ( $\epsilon_{280} = 1280 \text{ cm}^{-1} \text{ M}^{-1}$ ) using a 1 cm quartz cuvette (Hellma, Plainview, NY) and a Beckman DU-640 spectrophotometer (Beckman Instruments, Fullerton, CA). All measurements were performed at 22 °C. This protocol results in uniform and reproducible material termed low-molecular weight (LMW) A $\beta$ ,<sup>21</sup> containing monomeric A $\beta$  in equilibrium with low-order, unstructured oligomers. LMW A $\beta$  was cross-linked immediately upon preparation.

**Preparation of  $\alpha$ Syn and IAPP.** To prepare aggregate-free  $\alpha$ Syn and IAPP, the lyophilized peptide was dissolved with ice-cold HFIP and then dried in silicon-coated low-adsorbent tubes, as described previously.<sup>22</sup> These "protein films" were stored airtight at  $-20^\circ\text{C}$ . Prior to use, the peptide film was resolubilized, initially in 60 mM NaOH.<sup>22</sup>

**Photochemical Cross-Linking Using PICUP.** Immediately after preparation, peptide solutions were diluted to concentrations of 5–40  $\mu\text{M}$  and then cross-linked using the PICUP method, as described previously.<sup>19</sup> Briefly, 18  $\mu\text{L}$  of a protein solution was added to 1  $\mu\text{L}$  of 2 mM Ru(II)bpy<sub>3</sub><sup>2+</sup> and 1  $\mu\text{L}$  of 40 mM APS. The mixture was irradiated for 1 s with a 150 W visible light source, and the reaction was immediately quenched with 1  $\mu\text{L}$  of 1 M DTT. For each reaction, the mixture was vortexed for 1 s before and after addition of the



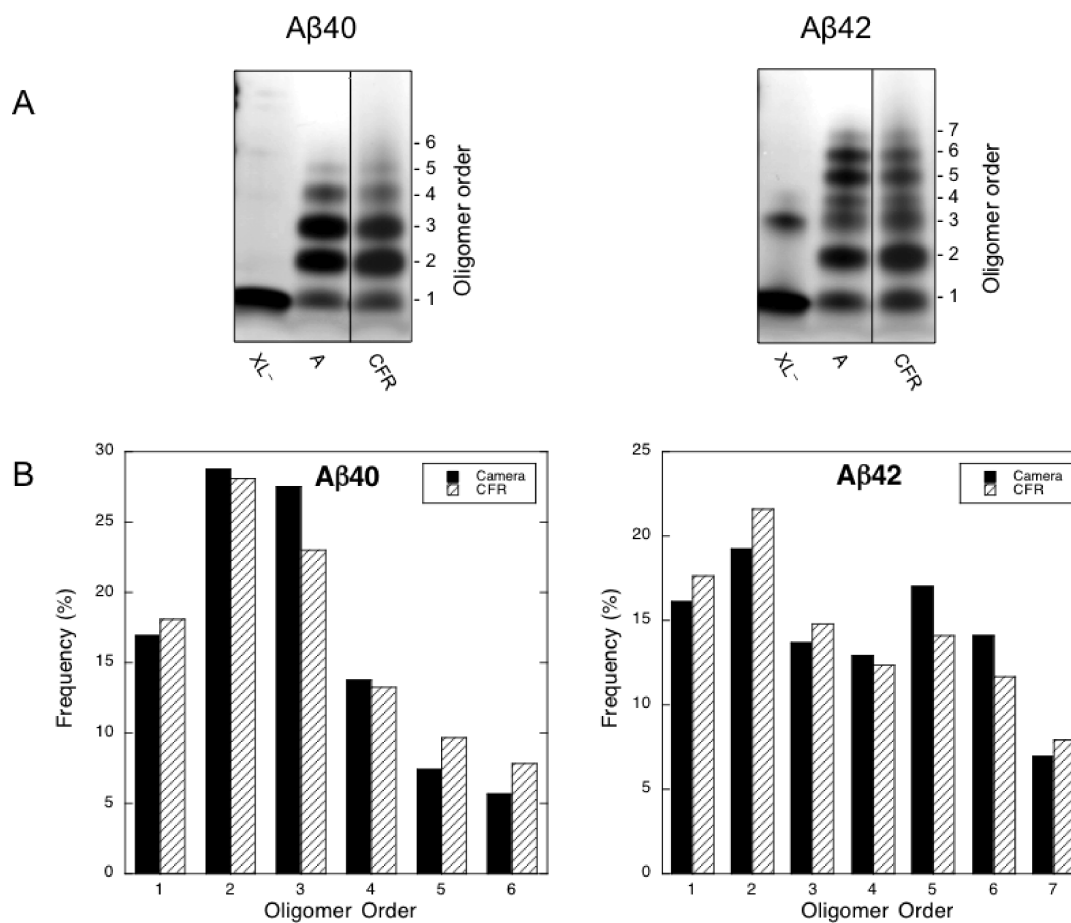


**Figure 4.** (A) Analytical vs continuous flow cross-linking of A $\beta$ 40 and A $\beta$ 42. The leftmost lanes contained non-cross-linked protein (XL<sup>-</sup>); the middle lanes show analytical-scale cross-linking (A), and the rightmost lanes show 0.2 mL/min continuous flow cross-linking (CFR) (these data from Figure 3 are shown here side by side for the sake of clarity of comparison). The number of monomers per oligomer is shown on the right. (B) Densitometry analysis of oligomer abundance for analytical vs continuous flow cross-linking. Oligomer order is plotted vs oligomer frequency. Black bars show the abundance from the analytical-scale system. White bars represent the abundance from the continuous flow system.

instrument in which each component of our prior analytical-scale single-reaction system<sup>32</sup> has been modified for continuous flow chemistry. The cross-linking chemistry proceeds at a negligible rate unless Ru(II)bpy<sub>3</sub><sup>2+</sup> is photooxidized; thus the peptide, Ru(II)bpy<sub>3</sub><sup>2+</sup> complex, and APS are premixed in a lighttight reservoir kept on ice. Premixing the reactants in this way eliminates the need for an even rudimentary online fluidic mixing device. The reactants are pumped through opaque (lighttight) tubing into an exposure chamber using a peristaltic pump, which allows precise control of flow rates, and thus irradiation time. The exposure chamber is a black box (literally) through which the tubing passes. A small opening is created in the box to allow the entrance of light from a 20 W tungsten halogen lamp. Various lamps will work. The primary lamp design consideration was photon flux, which determines irradiation time (flow rate), although cost and maneuverability are also considerations. To create an irradiation volume, a section of clear tubing was “spliced” into the tubing within the exposure chamber. The volume of the exposed sample was calculated to be 34.5  $\mu$ L (4.4 cm of 1 mm inside diameter tubing). This region of tubing was 6 cm from the light source. Quenching of the reaction is done by placing the outflow tube from the exposure chamber into a vessel containing 1 M dithiothreitol in water.

Because differences in irradiation time can affect the cross-linking efficiency, reproducibility requires that each element in

the reaction volume be irradiated identically. To determine if this was so, we calculated the Reynolds number of the system. The Reynolds number,<sup>33</sup>  $Re$ , is a dimensionless number that gives a measure of the ratio of inertial forces to viscous forces and thus can determine if fluid flow is laminar or turbulent. The instrument should display laminar flow so that the residence time of each molecule is constant. Using the equation

$$Re = \frac{\rho VD}{\mu}$$

where solvent density  $\rho = 1000 \text{ kg/m}^3$ , mean velocity  $V = 0.036545 \text{ m/s}$ , cylinder diameter  $D = 0.001 \text{ m}$ , and dynamic viscosity  $\mu = 8.98 \times 10^{-4} \text{ kg m}^{-1} \text{ s}^{-1}$ , we determined the Reynolds number to be between 30 and 40, which is far below the upper limit (2300) of the laminar flow regime. Thus, the geometry and flow rates for the CFR system described above will produce a laminar flow of the reactants, leading to homogeneous irradiation and consistent cross-linked products.

**Establishment of Operating Parameters. Temperature Control.** We found that heat radiating from the lamp caused an increase in the temperature of the illuminated tubing over time and, as a result, increased fluid temperatures and altered reaction rates. The distance from the light source to the irradiation site is proportional to the heating effect. To ensure a constant reaction temperature, we placed an infrared filter between the



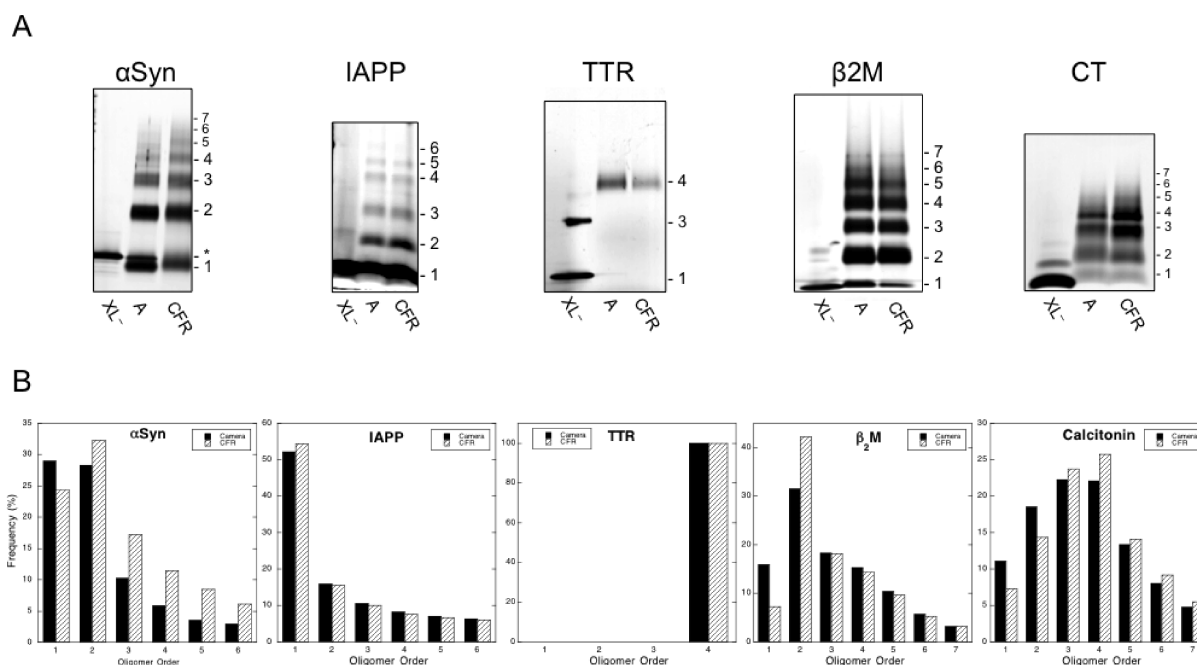


**Figure 5.** (A) Silver-stained SDS–PAGE analysis of analytical vs continuous flow cross-linking of  $\alpha$ Syn, IAPP, TTR,  $\beta$ 2M, and CT oligomers. For each peptide, the leftmost lanes contained non-cross-linked protein (XL<sup>-</sup>), the middle lanes show analytical-scale cross-linking (A), and the rightmost lanes show continuous flow cross-linking (CFR). The oligomer order is shown beside each distribution. (B) Densitometry analysis of oligomer abundance for analytical vs continuous flow cross-linking. Oligomer order is plotted vs oligomer frequency. Black bars show the abundance from the analytical-scale system. White bars represent the abundance from the continuous flow system.

lamp and the irradiated volume. This reduced the temperature increase (data not shown), although 4 °C water immediately came to room temperature (22–23 °C) upon flowing through the previously empty, room-temperature tubing of the CFR system. This temperature jump is likely due to the friction of the peristaltic pump and the transfer of heat from the room-temperature CFR tubing. We determined that we could equilibrate the reactor prior to use by pumping 4 °C water through the tubing for 10 min at a rate of 1 mL/min. After this equilibration process, a constant reaction temperature could be maintained.

**Irradiation Time Determination.** The CFR design allows control of irradiation time by simple adjustment of the flow rate. When the PICUP technique originally was adapted to the A $\beta$  system, we observed that short irradiation times resulted in inefficient cross-linking but long irradiation times resulted in peptide damage.<sup>19</sup> To establish optimal irradiation times for the CFR, we performed reactions at flow rates from 0.02 to 6.0 mL/min. We evaluated cross-linking quality by performing sodium dodecyl sulfate–polyacrylamide gel electrophoresis (SDS–PAGE) and silver staining on samples from each flow rate. “Quality” was determined by comparison of results from the CFR with those obtained using our camera-based method (Figure 3). At the fastest flow rate, 6.0 mL/min, the monomer is much more abundant than it is using the camera-based PICUP method, and fewer high-order oligomers are observed. This reflects lower cross-linking efficiency. There is a gradual decrease in the amount of monomer and a concomitant increase in the amounts of higher-order oligomers as the flow rate is decreased. At the slowest flow rates (longest exposure times), little or no monomer is observed and the oligomer distribution “collapses” into one comprising primarily dimer and trimer. In addition, the oligomer bands become more nebulous, likely because of the formation of multiple species (intra- and intermolecularly cross-linked) with similar molecular masses

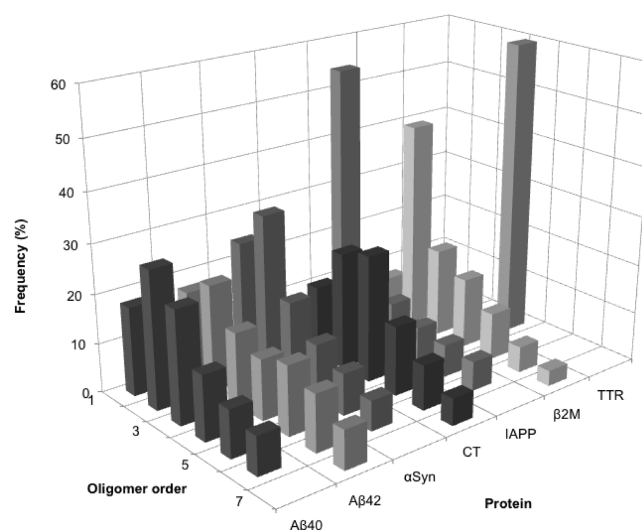


**Figure 6.** Oligomer frequency distributions of CFR products. For each protein, oligomer frequency (%) is plotted vs oligomer order. The % abundance axis is shown at 60% for the sake of clarity, though TTR is 100% tetramer.

but slightly different mobilities on SDS–PAGE. Bitan et al.<sup>19</sup> carefully described the effect of extended irradiation times on the relative abundance of A $\beta$  oligomers when initially characterizing the application of PICUP to A $\beta$ , concluding that irradiation time had little effect on the relative abundances of low-order oligomers. Our experiments revealed optimal flow rates to be between 0.2 and 1.0 mL/min (Figure 3). At these rates, cross-linking occurred efficiently without peptide damage. The calculated exposure time for a flow rate of 1 mL/min is 2 s. For the analytical-scale system, the typical exposure is 1 s. The longer exposure time for the CFR likely results from a combination of

**Table 1. Comparison of Time and Effort for Analytical versus Continuous Flow Cross-Linking<sup>a</sup>**

protein quantity	effort and time	analytical PICUP	continuous flow PICUP	analytical/CF ratio
1 $\mu$ g	effort	one individual reaction, four pipetting steps, one exposure	one reaction, four pipetting steps, one exposure of <1 min	1
	total time	2 min	2 min	1
1 mg	effort	100 individual reactions, 400 pipetting steps, 100 exposures	one reaction, four pipetting steps, one exposure of 2 min	100
	total time	200 min	4 min	50
1 g	effort	100000 individual reactions, 400000 pipetting steps, 100000 exposures, 600000 min of investigator time <sup>b</sup>	one reaction, four pipetting steps, one exposure of 2000 min, 2 min of investigator time	300000
	total time	$\approx$ 14 months	1.4 days of elapsed time	300

<sup>a</sup>Production capacity and its related metrics are shown for each method. The continuous flow apparatus allows for production of theoretically limitless quantities, while at the same time reducing investigator time by 4 orders of magnitude (for a 1 g preparation). Time and effort are shown for a flow rate of 1 mL/min and concentration of 0.5 mg/mL. <sup>b</sup>Total elapsed investigator time of 600000 min, assuming an 8 h work day (14 months).

the use of a weaker light source, 20 W, as compared to a power of 150 W, and the difference in system geometry.

**Comparison of CFR and Analytical-Scale Cross-Linking Methods.** To validate the CFR system relative to our analytical-scale camera system, we compared the A $\beta$ 40 and A $\beta$ 42 oligomer distributions (Figure 4). For each peptide, the two techniques produced similar distributions (lanes XL<sup>-</sup>, XL<sup>+</sup>, and 0.2 in Figure 3, shown side by side in Figure 4A). The CFR was marginally less efficient, as measured by monomer level. To compare the distributions quantitatively, we performed densitometry analyses using ImageJ (Figure 4B). The quantification showed that the CFR produced more higher-order oligomers for A $\beta$ 40, though this is potentially influenced by the smearing effect seen at the slowest flow rates (Figure 3). Quantification showed that dimer was the most abundant oligomer species for both A $\beta$ 40 and A $\beta$ 42. We observed monomer through hexamer oligomer states for A $\beta$ 40, and monomer through heptamer states for A $\beta$ 42. As expected,<sup>19</sup> the pentamer and hexamer states in the A $\beta$ 42 distribution constituted a node, though this node was slightly less pronounced with the CFR than with the analytical-scale system (17% vs 14% for pentamer and 14% vs 11.6% for hexamer).

**General Utility of the CFR.** The A $\beta$  system is not the only one in which oligomers exist or are thought to be important in disease causation. Proteins or peptides have been implicated in Parkinson's disease ( $\alpha$ Syn),<sup>9</sup> senile systemic amyloidosis and familial amyloid polyneuropathy (TTR),<sup>12</sup> dialysis-related amyloidosis ( $\beta$ 2M),<sup>13</sup> and medullary carcinoma of the thyroid (CT),<sup>14</sup> among others.<sup>13</sup> To determine whether the CFR might be of use for the preparation of large quantities of chemically stabilized oligomers of these other proteins, we cross-linked  $\alpha$ Syn, IAPP, TTR,  $\beta$ 2M, and CT and compared the resulting oligomer distributions with those obtained after cross-linking 5–10  $\mu$ g of each protein using the analytical-scale PICUP method. In each system, PICUP was performed immediately upon protein dissolution (Figure 5A).

We found, as in the A $\beta$ 40 and A $\beta$ 42 cases, that the oligomer populations produced using each method were qualitatively similar or identical, within experimental error (cf. "A" and "CFR" for each sample). Densitometry analyses were consistent with this conclusion but also suggested, in the cases of  $\alpha$ Syn,  $\beta$ 2M, and CT, that the CFR method was more efficient (Figure 5B). This could be inferred by relative decreases in monomer frequency and increases in the frequency of higher-order oligomers upon comparison of the CFR results to those from the analytical-scale method.

We note that the most abundant oligomer species for  $\alpha$ Syn and  $\beta$ 2M was dimer. IAPP exhibited abundant monomer, followed by a sharp decrease in oligomer abundance as oligomer order increased. Interestingly, the oligomer distribution for IAPP resembled that predicted for high-efficiency cross-linking of proteins undergoing random diffusion-limited collisions,<sup>19</sup> suggesting that substantial oligomerization had not occurred in the  $\approx$ 4 min required to dissolve and cross-link IAPP. Cross-linked TTR displayed only tetramer and a very nebulous dimer band, whereas CT showed a Gaussian-like distribution of oligomers centered at trimer and tetramer. A three-dimensional representation of the oligomer abundance profiles for each protein illustrates these similarities and differences (Figure 6).

## DISCUSSION

One major obstacle to a detailed understanding of A $\beta$  oligomer structure and activity is the diversity and complexity of oligomer preparation methods, and the widespread use of poorly defined materials derived therefrom in studies of the effects of oligomers. A critical aspect of the CFR method is that it reliably produces consistent starting material with stability far superior to that of non-cross-linked oligomer preparations and in quantities sufficient for examination by myriad *in vitro*, *ex vivo*, and *in vivo* methods. These include studies of the effects of oligomers on cellular pathways (inflammation and signaling), animal models of disease, structural studies (CD, TEM, AFM, NMR, and crystallography), and effects on gene expression. Importantly, the CFR is a simple yet powerful device that can easily be fabricated. To assemble a CFR, a laboratory needs to have only (1) a peristaltic pump, (2) a light source (as basic as a flashlight<sup>28</sup>), and (3) tubing.

Oligomer structure cannot be studied formally, at present, in the absence of oligomer stabilization. In fact, the difficulty in studying unstabilized oligomers has been a significant barrier to progress in the field. Even if one begins an experiment with an oligomer "enriched" fraction, the results thus obtained represent "population average" data because the oligomer fraction exists in an equilibrium among many different species. One cannot determine the structure of a particular oligomer and how that oligomer contributes to this population average for any particular biological effect. Structure–activity relationships of A $\beta$  oligomers thus have not been established without stabilization (see ref 17).

The inability to determine the structures of unstabilized oligomers precludes a comparison of their structures with those

of chemically stabilized oligomers. However, there are reasons to suggest that they may be very similar. The oligomers differ in primary structure only through the presence or absence of the carbon–carbon bond in the zero-length cross-linking procedure. No alterations in the solvent milieu of the peptides are made during the cross-linking. In addition, we have found that A $\beta$ 40 and A $\beta$ 42 monomers do exist in a partially folded state.<sup>34</sup> This means, prior to cross-linking, that the conformational space of the oligomer population is relatively restricted and thus if that state is stabilized properly, it would be representative of the population of conformers at the time of cross-linking.

The benefit of the CFR could be far-reaching in the general field of oligomer study. The reactor allows the study of the properties of chemically stabilized oligomers not only of A $\beta$  but also of  $\alpha$ Syn,  $\beta$ 2M, IAPP, and CT. The CFR method thus is not restricted to the study of any one protein or disease but can be applied broadly to many diseases in which oligomers may be involved.

Finally, a very significant practical advantage is provided by the CFR, namely time–effort efficiency (Table 1). Analytical-scale reactions each typically involve 20  $\mu$ L of 80  $\mu$ M A $\beta$  (10  $\mu$ g). In the continuous flow reactor, the quantity of sample is limited only by the amount of protein available. For example, producing 1 mg of cross-linked protein using the analytical method would require 100 individual reactions, 400 individual pipetting steps, and turning the light source on and off (actuating the shutter release) 100 times to irradiate the samples, a total of  $\approx$ 200 min of investigator time. In contrast, using the CFR system, the entire 1 mg is produced in one step, at a rate of 1 mL/min, with only four pipetting steps, with the lamp on for 1 min, finishing the reaction in  $\approx$ 4 min, a 50-fold time savings. This time-effort efficiency becomes more dramatic when considering the production of larger volumes. It would take  $\approx$ 200000 min of investigator time to prepare 1 g of sample with the analytical method. If this time were expended during an 8 h work day, the entire process then would take 14 months. In contrast, using the CFR system, preparing 1 g would take just 2000 min (33 h) of total time, with only 2 min of investigator time input, a 300000-fold savings in investigator time and a 300-fold savings in elapsed time.

## AUTHOR INFORMATION

### Corresponding Author

\*Phone: (310) 206-2030. E-mail: dteplow@ucla.edu.

### Author Contributions

E.Y.H. and D.B.T. designed the experiments. E.Y.H. performed the experiments. E.Y.H. and D.B.T. wrote the manuscript.

### Funding

This work was supported by National Institutes of Health Grants NF038328 and ST32NS07449.

### Notes

The authors declare no competing financial interest.

## ACKNOWLEDGMENTS

We thank Drs. Gal Bitan, Robin Roychaudhuri, Mingfeng Yang, Dahabada Lopes, and Ghiam Yamin for helpful comments and discussion. We thank Margaret Condon for synthesis of A $\beta$ .

## ABBREVIATIONS

AD, Alzheimer's disease; A $\beta$ , amyloid  $\beta$ -protein;  $\alpha$ Syn,  $\alpha$ -synuclein; IAPP, islet amyloid polypeptide; TTR, transthyretin;  $\beta$ 2M,  $\beta$ 2-microglobulin; CT, calcitonin; SAR, structure–activity

relationship(s); PICUP, photoinduced cross-linking of unmodified proteins; Ru(II)bpy<sub>3</sub><sup>2+</sup>, tris(2,2'-bipyridyl)ruthenium(II) chloride hexahydrate; APS, ammonium persulfate; CFR, continuous flow reactor; XL<sup>−</sup>, non-cross-linked; XL<sup>+</sup>, cross-linked.

## REFERENCES

- (1) Alzheimer's Disease International (2010) World Alzheimer's Report.
- (2) Brookmeyer, R., Johnson, E., Ziegler-Graham, K., and Arrighi, H. M. (2007) Forecasting the global burden of Alzheimer's disease. *Alzheimer's Dementia* 3, 186–191.
- (3) Roychaudhuri, R., Yang, M., Hoshi, M. M., and Teplow, D. B. (2009) Amyloid  $\beta$ -protein assembly and Alzheimer disease. *J. Biol. Chem.* 284, 4749–4753.
- (4) De Meyer, G., Shapiro, F., Vanderstichele, H., Vanmechelen, E., Engelborghs, S., De Deyn, P. P., Coart, E., Hansson, O., Minthon, L., Zetterberg, H., Blennow, K., Shaw, L., and Trojanowski, J. Q. (2010) Diagnosis-independent Alzheimer disease biomarker signature in cognitively normal elderly people. *Arch. Neurol.* 67, 949–956.
- (5) Kawarabayashi, T., Shoji, M., Younkin, L. H., Wen-Lang, L., Dickson, D. W., Murakami, T., Matsubara, E., Abe, K., Ashe, K. H., and Younkin, S. G. (2004) Dimeric amyloid  $\beta$  protein rapidly accumulates in lipid rafts followed by apolipoprotein E and phosphorylated tau accumulation in the Tg2576 mouse model of Alzheimer's disease. *J. Neurosci.* 24, 3801–3809.
- (6) Näslund, J., Haroutunian, V., Mohs, R., Davis, K. L., Davies, P., Greengard, P., and Buxbaum, J. D. (2000) Correlation between elevated levels of amyloid  $\beta$ -peptide in the brain and cognitive decline. *JAMA, J. Am. Med. Assoc.* 283, 1571–1577.
- (7) Walsh, D. M., Klyubin, I., Fadeeva, J. V., Cullen, W. K., Anwyl, R., Wolfe, M. S., Rowan, M. J., and Selkoe, D. J. (2002) Naturally secreted oligomers of amyloid  $\beta$ -protein potently inhibit hippocampal long-term potentiation in vivo. *Nature* 416, 535–539.
- (8) Walsh, D. M., and Selkoe, D. J. (2007) A $\beta$  oligomers: A decade of discovery. *J. Neurochem.* 101, 1172–1184.
- (9) Winner, B., Jappelli, R., Maji, S. K., Desplats, P. A., Boyer, L., Aigner, S., Hetzer, C., Loher, T., Vilar, M., Campioni, S., Tzitzilonis, C., Soragni, A., Jessberger, S., Mira, H., Consiglio, A., Pham, E., Masliah, E., Gage, F. H., and Riek, R. (2011) In vivo demonstration that  $\alpha$ -synuclein oligomers are toxic. *Proc. Natl. Acad. Sci. U.S.A.* 108, 4194–4199.
- (10) Gurlo, T., Ryazantsev, S., Huang, C. J., Yeh, M. W., Reber, H. A., Hines, O. J., O'Brien, T. D., Glabe, C. G., and Butler, P. C. (2010) Evidence for proteotoxicity in  $\beta$  cells in type 2 diabetes: Toxic islet amyloid polypeptide oligomers form intracellularly in the secretory pathway. *Am. J. Pathol.* 176, 861–869.
- (11) Haataja, L., Gurlo, T., Huang, C. J., and Butler, P. C. (2008) Islet amyloid in type 2 diabetes, and the toxic oligomer hypothesis. *Endocr. Rev.* 29, 303–316.
- (12) Sorgjerd, K., Klingstedt, T., Lindgren, M., Kagedal, K., and Hammarstrom, P. (2008) Prefibrillar transthyretin oligomers and cold stored native tetrameric transthyretin are cytotoxic in cell culture. *Biochem. Biophys. Res. Commun.* 377, 1072–1078.
- (13) Kad, N. M., Myers, S. L., Smith, D. P., Alastair Smith, D., Radford, S. E., and Thomson, N. H. (2003) Hierarchical assembly of  $\beta$ 2-microglobulin amyloid *in vitro* revealed by atomic force microscopy. *J. Mol. Biol.* 330, 785–797.
- (14) Arvinte, T., Cudd, A., and Drake, A. F. (1993) The structure and mechanism of formation of human calcitonin fibrils. *J. Biol. Chem.* 268, 6415–6422.
- (15) Teplow, D. B. (2006) Preparation of amyloid  $\beta$ -protein for structural and functional studies. *Methods Enzymol.* 413, 20–33.
- (16) Hayden, E. Y., and Teplow, D. B. (2012) Biophysical characterization of A $\beta$  assembly. In *Alzheimer's Disease: Insights into low molecular weight and cytotoxic aggregates from in vitro and computer experiments: Molecular Basis of Amyloid- $\beta$  Protein Aggregation and Fibril Formation* (Derreumaux, P., Ed.) Imperial College Press, London, in press.

- (17) Ono, K., Condrón, M. M., and Teplow, D. B. (2009) Structure-neurotoxicity relationships of amyloid  $\beta$ -protein oligomers. *Proc. Natl. Acad. Sci. U.S.A.* 106, 14745–14750.
- (18) Bitan, G., and Teplow, D. B. (2004) Rapid photochemical cross-linking: A new tool for studies of metastable, amyloidogenic protein assemblies. *Acc. Chem. Res.* 37, 357–364.
- (19) Bitan, G., Lomakin, A., and Teplow, D. B. (2001) Amyloid  $\beta$ -protein oligomerization: Prenucleation interactions revealed by photo-induced cross-linking of unmodified proteins. *J. Biol. Chem.* 276, 35176–35184.
- (20) Urbanc, B., Cruz, L., Yun, S., Buldyrev, S. V., Bitan, G., Teplow, D. B., and Stanley, H. E. (2004) In silico study of amyloid  $\beta$ -protein folding and oligomerization. *Proc. Natl. Acad. Sci. U.S.A.* 101, 17345–17350.
- (21) Walsh, D. M., Hartley, D. M., Kusumoto, Y., Fezoui, Y., Condrón, M. M., Lomakin, A., Benedek, G. B., Selkoe, D. J., and Teplow, D. B. (1999) Amyloid  $\beta$ -protein fibrillogenesis. Structure and biological activity of protofibrillar intermediates. *J. Biol. Chem.* 274, 25945–25952.
- (22) Rahimi, F., Maiti, P., and Bitan, G. (2009) Photo-induced cross-linking of unmodified proteins (PICUP) applied to amyloidogenic peptides. *J. Visualized Exp.* 23, e1071.
- (23) Teplow, D. B., Lazo, N. D., Bitan, G., Bernstein, S., Wyttenbach, T., Bowers, M. T., Baumketner, A., Shea, J. E., Urbanc, B., Cruz, L., Borreguero, J., and Stanley, H. E. (2006) Elucidating amyloid  $\beta$ -protein folding and assembly: A multidisciplinary approach. *Acc. Chem. Res.* 39, 635–645.
- (24) Nickel, U., Chen, Y.-H., Schneider, S., Silva, M. I., Burrows, H. D., and Formosinho, S. J. (1994) Mechanism and kinetics of the photocatalyzed oxidation of p-phenylenediamines by peroxydisulfate in the presence of tri-2,2'-bipyridylruthenium(II). *J. Phys. Chem.* 98, 2883–2888.
- (25) Gray, H. B., and Winkler, J. R. (1996) Electron transfer in proteins. *Annu. Rev. Biochem.* 65, 537–561.
- (26) Yocom, K. M., Shelton, J. B., Shelton, J. R., Schroeder, W. A., Worosila, G., Isied, S. S., Bordignon, E., and Gray, H. B. (1982) Preparation and characterization of a pentaammineruthenium(III) derivative of horse heart ferricytochrome c. *Proc. Natl. Acad. Sci. U.S.A.* 79, 7052–7055.
- (27) Berglund, J., Pascher, T., Winkler, J. R., and Gray, H. B. (1997) Photoinduced oxidation of horseradish peroxidase. *J. Am. Chem. Soc.* 119, 2464–2469.
- (28) Fancy, D. A., and Kodadek, T. (1999) Chemistry for the analysis of protein-protein interactions: Rapid and efficient cross-linking triggered by long wavelength light. *Proc. Natl. Acad. Sci. U.S.A.* 96, 6020–6024.
- (29) Fancy, D. A., Denison, C., Kim, K., Xie, Y., Holdeman, T., Amini, F., and Kodadek, T. (2000) Scope, limitations and mechanistic aspects of the photo-induced cross-linking of proteins by water-soluble metal complexes. *Chem. Biol.* 7, 697–708.
- (30) Das, M., and Fox, C. F. (1979) Chemical cross-linking in biology. *Annu. Rev. Biophys. Bioeng.* 8, 165–193.
- (31) Knorre, D. G., and Godovikova, T. S. (1998) Photoaffinity labeling as an approach to study supramolecular nucleoprotein complexes. *FEBS Lett.* 433, 9–14.
- (32) Vollers, S. S., Teplow, D. B., and Bitan, G. (2005) Determination of peptide oligomerization state using rapid photochemical crosslinking. *Methods Mol. Biol.* 299, 11–18.
- (33) Reynolds, O. (1883) An experimental investigation of the circumstances which determine whether the motion of water shall be direct or sinuous, and of the law of resistance in parallel channels. *Philos. Trans. R. Soc. London* 174, 935–982.
- (34) Grant, M. A., Lazo, N. D., Lomakin, A., Condrón, M. M., Arai, H., Yamin, G., Rigby, A. C., and Teplow, D. B. (2007) Familial Alzheimer's disease mutations alter the stability of the amyloid  $\beta$ -protein monomer folding nucleus. *Proc. Natl. Acad. Sci. U.S.A.* 104, 16522–16527.